

## Supplementary Materials

### **Uncertainties in assessing the environmental impact of amine emissions from a CO<sub>2</sub> capture plant**

Matthias Karl<sup>1,\*</sup>, Nuria Castell<sup>1</sup>, David Simpson<sup>3,4</sup>, Sverre Solberg<sup>1</sup>, Jostein Starrfelt<sup>2</sup>, Tove Svendby<sup>1</sup>, Sam-Erik Walker<sup>1</sup>, and Richard F. Wright<sup>2</sup>

[1] Norwegian Institute for Air Research, NILU, Instituttveien 18, 2027 Kjeller, Norway

[2] Norwegian Institute for Water Research, NIVA, Gaustadalléen 21, 0349 Oslo, Norway

[3] EMEP MSC-W, Norwegian Meteorological Institute, Oslo, Norway

[4] Dept. Earth & Space Sciences, Chalmers Univ. Technology, Gothenburg, Sweden

\* Corresponding author: [mka@nilu.no](mailto:mka@nilu.no)

## S1. Gridded emissions in the EMEP model

The standard emissions input to the EMEP model is gridded national annual emissions of sulphur oxides ( $\text{SO}_x = \text{SO}_2 + \text{SO}_4$ ), nitrogen oxides ( $\text{NO}_x = \text{NO} + \text{NO}_2$ ), ammonia ( $\text{NH}_3$ ), non-methane volatile organic compounds (NMVOC), carbon monoxide (CO), and particulates ( $\text{PM}_{2.5}$ ,  $\text{PM}_{10}$ ) (<http://www.ceip.at>). The traditional EMEP model has a spatial resolution of 50 km, but here we have used an emission inventory based on TNO-MACC (Kuenen et al., 2011) with spatial resolution of  $1/8 \times 1/16$  lon-lat (approximately  $7 \times 7 \text{ km}^2$ ), rescaled to match the official EMEP 2009 country total emissions. The dataset, hereafter denoted TNO7, was delivered by INERIS for the "TFMM Scale Dependency Study" (Schaap et al., 2012). Details of the treatment of such emissions in the EMEP model (including speciation, time-variation, etc.) are given in Simpson et al. (2012). Even these TNO7 emissions have coarser resolution compared to the  $2 \times 2 \text{ km}^2$  model grid. In order to make the power plant emission as realistic as possible, the TNO7 data were first reallocated to a finer 2 km grid, with similar projection and size as the inner model domain. Next, the redistributed emissions in approximately 10 km distance from Mongstad were replaced by representative background values, whereas the excess emission was reallocated to the single  $2 \times 2 \text{ km}^2$  grid enclosing the Mongstad refinery and the power plant.

Total  $\text{NO}_x$  area emission in the grid cell of Mongstad was 260 Mg per year (SNAP category 1: Combustion in energy and transformation industries). The total  $\text{NO}_x$  emission in the Mongstad grid cell from area and point sources for the year 2007 was reported by Statoil Mongstad to be  $1930 \text{ Mg yr}^{-1}$  as registered in the European Pollutant Release and Transfer Register (<http://prtr.ec.europa.eu>). The contribution from the power plant is estimated to be  $140 \text{ Mg yr}^{-1}$  based on data by Statoil Mongstad for 2007 (see **Table S3**). It is assumed that the installation of the CCP does not affect the  $\text{NO}_x$  emissions of the power plant.

## S2. Plume rise treatment in the EMEP model

Three options for plume rise calculation for point sources have been implemented into the EMEP model. The option ‘NILU plume’ takes into account different boundary layer stability conditions, where the inverse Obukhov length is used to characterize the boundary layer stability, and follows the plume rise description by Briggs (e.g. Briggs, 1971) with modifications. The option ‘ASME Plume’ is adequate for buoyant plumes and calculates final plume rise for neutral and stable conditions using a simplified parameterization, with exhaust gas volume flow rate as main control parameter (ASME 1973; Seinfeld and Pandis, 1998). The option ‘PVDI Plume’ is adequate for large point sources and calculates plume rise according to the German VDI Guideline 3782 Part 3 (VDI, 1985) considering parameterizations for different temperature stratifications and heat fluxes based on plume rise equations by Briggs (1971) with modifications for neutral temperature stratification (Pregger and Friedrich, 2009). Emitted heat flux (in MW) is the main control parameter in the ‘PVDI Plume’ parameterization, which is proportional to exhaust gas volume flow rate and temperature difference between exhaust gas and ambient air temperature.

Final plume rise ( $\Delta h_f$ ) calculated by the three plume rise methods was compared for a generic stack with exhaust gas temperature of 313.15 K and ambient air temperature of 283.15 K. Three test series were performed: (1) variation of stack height ( $H_s$ ) between 50 and 90 m; (2) variation of exit velocity ( $V_s$ ) between 5 and 13 m s<sup>-1</sup>; and (3) variation of diameter ( $D$ ) between 2.5 and 6.5 m. For ‘NILU Plume’, a stable condition ( $L = 20$  m), an unstable condition ( $L = -10$  m) and a neutral condition ( $L = 10^6$  m) were tested. For ‘ASME Plume’ both a stable condition ( $dT/dz = 0.10$  K m<sup>-1</sup>) and a neutral condition ( $dT/dz = -0.01$  K m<sup>-1</sup>) were tested. **Table S4** summarizes the final plume rise results obtained from this test. For all tested parameter sets, ‘NILU Plume’ resulted in the lowest plume rise. The low final plume rise of the ‘NILU Plume’ parameterization can be explained by the decision flow of the plume rise algorithm - illustrated in **Figure S1** - which tends to select low values for final plume rise. For example, the lower of the stable momentum rise and neutral-unstable momentum rise is chosen as final plume rise. ‘ASME Plume’ results were within a factor of 2 similar to the ‘NILU Plume’ results for stable condition, but up to 8 times higher than the ‘NILU Plume’ results for neutral condition. For the given ranges of variation, calculated final plume rise was most sensitive to changes in stack diameter. ‘ASME Plume’ for neutral condition gave the highest plume rise (147 m) in the test, for the largest diameter  $D = 6.5$  m. For the stack configuration of this study ( $H_s = 60$  m,  $D = 7.14$  m,  $V_s = 10$  m s<sup>-1</sup>) ‘ASME Plume’ (neutral) and ‘PVDI Plume’ gave similar results, with final plume rise of about 220 m.

### S3. Comparison of WRF meteorology to met station data

The WRF model was initialized with two datasets of meteorological initial and boundary conditions: ECMWF reanalysis data and NCEP FNL global analysis data. WRF model with both initializations was compared to local meteorological observation data in the region of Bergen at the West coast of Norway.

Comparison of wind roses for the stations Fedje, Bergen-Florida, Takle, Kvamskogen and Flesland for year 2007 in general shows good agreement between the WRF model (based on NCEP FNL data and on ECMWF data) and observations. Wind roses generated from the two model datasets were quite similar both in terms of frequency of wind direction and magnitude of wind speed. As an example, **Figure S2a - c** shows the annual wind rose based on measured data, WRF model with ECMWF data, and WRF model with NCEP FNL data at Fedje station, an island 18 km to the West of Mongstad. At Takle station (61.03°N; 5.39°E; 38 m a.s.l.), the WRF model for both NCEP FNL and ECMWF data overestimated the frequency of winds from southerly directions. The wind rose at the Norwegian west coast in the Bergen region changes throughout the year, with a clear prevalence of E-SE winds in winter and a higher frequency of NW winds in summer (**Fig. S2d-f**). During autumn and spring the components from SE to N are more frequent, with prevailing Atlantic winds.

The pattern of wind direction and wind speed throughout the year is reproduced at the stations Bergen, Takle, Fedje and Kvamskogen well by the WRF model (**Figure S3**). At Fedje, which is frequently exposed to strong winds, even high wind speeds were captured well. WRF tended to underestimate the wind speed of the strong winds with measured wind speed  $>10 \text{ m s}^{-1}$ . On the other hand, WRF overestimated wind speeds at the inland site Kvamskogen, although it captured the pattern reasonably well. Unfortunately, none of these stations is exactly representative for the conditions at the location of the Mongstad refinery.

On the basis of daily averages, the agreement between observed temperature and modelled temperature was excellent at the stations Fedje, Flesland, Kvamskogen, and Takle, both in terms of variation and in terms of absolute values (**Figure S4**). The WRF model was capable of accurately reproducing ground air temperatures and temperature variations in the region of Mongstad during 2007. Modelled daily and monthly average temperature from the two meteorological datasets - ECMWF and NCEP FNL - was in close agreement, not deviating by more than 1°C at the four stations.

**Table S1:** Physiochemical characteristics of the two nitrosamines and two nitramines for which the Fugacity III model was applied (adopted from Yiannoukas, 2011). MW: molecular weight; Kow: octanol-water partition coefficient; Koc: organic carbon partition coefficient between liquid and solid phases; DT50: degradation time (ultimate) for 50% of the substance.

Compound group	MW (g mol <sup>-1</sup> )	Water sol. (mg l <sup>-1</sup> )	Vapor press. (mm Hg)	Melt point (°C)	Log Kow	Koc (l kg <sup>-1</sup> )	DT50 water days	DT50 soil days	DT50 sedim. days	DT50 atmos. days
Nitrosamine-2 (NDMA) Nitrosodimethyl amine	74	1x10 <sup>6</sup>	2.7	25	-0.57	0.110	23	38	207	4.2
Nitramine-1 Methyl-nitramine	76	1x10 <sup>6</sup>	6.99	38	-1.51	0.013	15	30	135	8.5
Nitramine-2 N,N dimethyl- nitramine	90	1x10 <sup>6</sup>	0.361	58	-0.52	0.124	15	30	135	2.8

**Table S2:** Physical parameters for the generic soil and lake used in the simulations for which the Fugacity III model was applied. MTC: mass transfer coefficient.

	Units	Value
<b>Catchment parameters</b>		
Area (ex. lake)	km <sup>2</sup>	1.95
Mean soil depth	m	10
Soil organic C	g/g	0.14
<b>Runoff parameters</b>		
Discharge	m/yr	1.7
Suspended particles	%vol	0.0005
Susp. particles organic C	g/g	0.14
<b>Lake parameters</b>		
Area	km <sup>2</sup>	0.16
Mean depth	m	10
Volume	mill. m <sup>3</sup>	1.6
Water retention time	yr	0.45
Sediment organic C	g/g	0.028
<b>Transport velocities</b>		
Air side air-water MTC	m/yr	43800
Water side air-water MTC	m/yr	438
Rain rate	m/yr	1.9
Aerosol dry deposition velocity	m/yr	0.000005256
Soil air phase diffusion MTC	m/yr	175.2
Soil water phase diffusion MTC	m/yr	0.0876
Soil air boundary layer MTC	m/yr	43800
Sediment-water MTC	m/yr	0.0876
Sediment deposition velocity	m/yr	0.00438
Sediment resuspension velocity	m/yr	0.001752
Soil water runoff rate	m/yr	1.7
Soil solids runoff rate	m/yr	0.0005256

**Table S3:** NO<sub>x</sub> emissions (in Mg per year) at Mongstad in the EMEP model.

Source	Refinery combustion (Area source)	Refinery (Point source, 103m stack)	Refinery (Point source, 50m stack)	CCP and power plant (Point source)	Total (w/o CCP)	Total (w CCP)
NO <sub>x</sub> emission (Mg per year)	260	940	590	140	1790	1930

**Table S4:** Final plume rise,  $\Delta h$ , (in m) calculated using the three plume rise options available in the EMEP model: ‘NILU Plume’, ‘ASME Plume’ and ‘PVDI Plume’ for exhaust gas temperature of 313.15 K, air temperature of 283.15 K, and wind speed of 2.5 m s<sup>-1</sup>.

Stack configuration	NILU Plume <i>neutral</i>	NILU Plume <i>unstable</i>	NILU Plume <i>stable</i>	ASME Plume <i>stable</i>	ASME Plume <i>neutral</i>	PVDI Plume
Hs=90 m, D=2.5 m, Vs=5 m s <sup>-1</sup>	15	15	15	27	115	35
Hs=70 m, D=2.5 m, Vs=5 m s <sup>-1</sup>	15	15	15	27	97	35
Hs=50 m, D=2.5 m, Vs=13 m s <sup>-1</sup>	39	39	39	38	107	64
Hs=50 m, D=2.5 m, Vs=11 m s <sup>-1</sup>	33	33	33	36	101	57
Hs=50 m, D=2.5 m, Vs=9 m s <sup>-1</sup>	27	27	27	33	95	49
Hs=50 m, D=2.5 m, Vs=7 m s <sup>-1</sup>	23	23	21	31	87	40
Hs=50 m, D=6.5 m, Vs=5 m s <sup>-1</sup>	54	53	39	52	147	129
Hs=50 m, D=5.5 m, Vs=5 m s <sup>-1</sup>	45	44	33	46	132	102
Hs=50 m, D=4.5 m, Vs=5 m s <sup>-1</sup>	36	36	27	41	115	76
Hs=50 m, D=3.5 m, Vs=5 m s <sup>-1</sup>	26	26	21	34	97	52
Hs=50 m, D=2.5 m, Vs=5 m s <sup>-1</sup>	18	18	17	27	78	35
Hs=60 m, D=7.14 m, Vs=10 m s <sup>-1</sup>	86	86	86	69	223	218

**Table S5:** Henry's Law coefficients for the aqueous phase partitioning in the EMEP model.

Compound	Chemical name	H (mol kg <sup>-1</sup> atm <sup>-1</sup> )	Reference
MEA	2-aminoethanol	6.18x10 <sup>6</sup>	Ge et al. (2011)
MEA-nitramine	2-nitro aminoethanol	1.42x10 <sup>7</sup>	EPI Suite, Bond method
DEYA	Diethylamine	132	Ge et al. (2011)
DEYA-nitramine	N-nitro diethylamine	178	EPI Suite, Bond method
DEYA-nitrosamine	N-nitroso diethylamine	275	Mirvish et al. (1976)

**Table S6:** Geographical location, availability and frequency of meteorological observations at the met stations in the Bergen region.

Station/ WMO no.	Station Name / County	Latitude Longitude Altitude	Observations			
			Wind	Temp.	RH	Precip.
52535 / 307	<b>Fedje</b> / Hordaland	60.780, 4.720, 19 m	6 h	6 h	6 h	
50310 / 327	<b>Kvamskogen</b> Jonshøgdi / Hordaland	60.389, 5.964, 455 m	6 h	6 h	6 h	
50540 / 317	<b>Bergen-Florida</b> / Hordaland	60.383, 5.334, 12 m	6 h	6 h	6 h	12 h
50500 / 311	<b>Flesland</b> / Hordaland	60.289, 5.227, 48 m	6 h	6 h	6 h	12 h
52860 / 319	<b>Takle</b> / Sogn i Fjordane	61.027, 5.385, 38 m	6 h *	6 h *	6 h *	12 h
52290 / 325	<b>Modalen II</b> / Hordaland	60.841, 5.953, 114 m	6 h *	6 h *	6 h *	12 h
56400	<b>Yttre Solund</b> / Sogn og Fjordane	61.005, 4.676, 3 m				24 h
56320	<b>Lavik</b> / Sogn og Fjordane	61.112, 5.547, 31 m				24 h
52930	<b>Brekke</b> / Sogn og Fjordane	60.959, 5.427, 240 m				24 h
52601	<b>Haukeland-</b> Storevatn / Hordaland	60.835, 5.583, 325 m				24 h
52750	<b>Frøyset</b> / Hordaland	60.848, 5.217, 13 m				24 h
52400	<b>Eikanger-Myr</b> / Hordaland	60.623, 5.381, 72 m				24 h

\* Only monitored at 7, 13, 19 GMT.



**Table S7:** Comparison of maximum monthly values of mean air concentration, dry deposition and wet deposition of an inert tracer (emission of 1 g/s) in a  $40 \times 40 \text{ km}^2$  domain around Mongstad computed by the TAPM model and by the WRF-EMEP model (using ECMWF meteorology).

Month in 2007	Air Concentration Max. value (in $40 \times 40 \text{ km}^2$ ) unit: $\text{ng/m}^3$		Dry Deposition Max. value (in $40 \times 40 \text{ km}^2$ ) unit: $\text{mg/m}^2$		Wet Deposition Max. value (in $40 \times 40 \text{ km}^2$ ) unit: $\text{mg/m}^2$	
	WRF- EMEP	TAPM	WRF- EMEP	TAPM	WRF- EMEP	TAPM
January	33	34	0.92	1.12	1.7	2.7
February	127	84	3.11	0.09	1.3	2.4
March	86	43	1.57	0.17	1.5	2.2
April	41	39	2.19	0.20	1.2	3.2
May	56	60	2.37	0.32	0.7	2.7
June	144	144	4.75	0.28	0.3	3.5
July	86	48	2.73	0.43	2.1	6.0
August	38	45	2.36	0.34	0.7	3.4
September	23	33	2.17	0.19	1.1	3.1
October	41	112	2.51	0.11	1.5	4.0
November	90	63	2.39	0.09	1.3	3.7
December	68	74	3.57	0.87	1.3	3.1

Both models used the following stack characteristics. Stack height: 60 m, stack diameter: 7.14 m, exit velocity: 10 m/s, and exhaust gas temperature: 313 K. Emission of inert tracer at  $1 \text{ g s}^{-1}$ .

## Logic Diagram for 'NILU Plume'

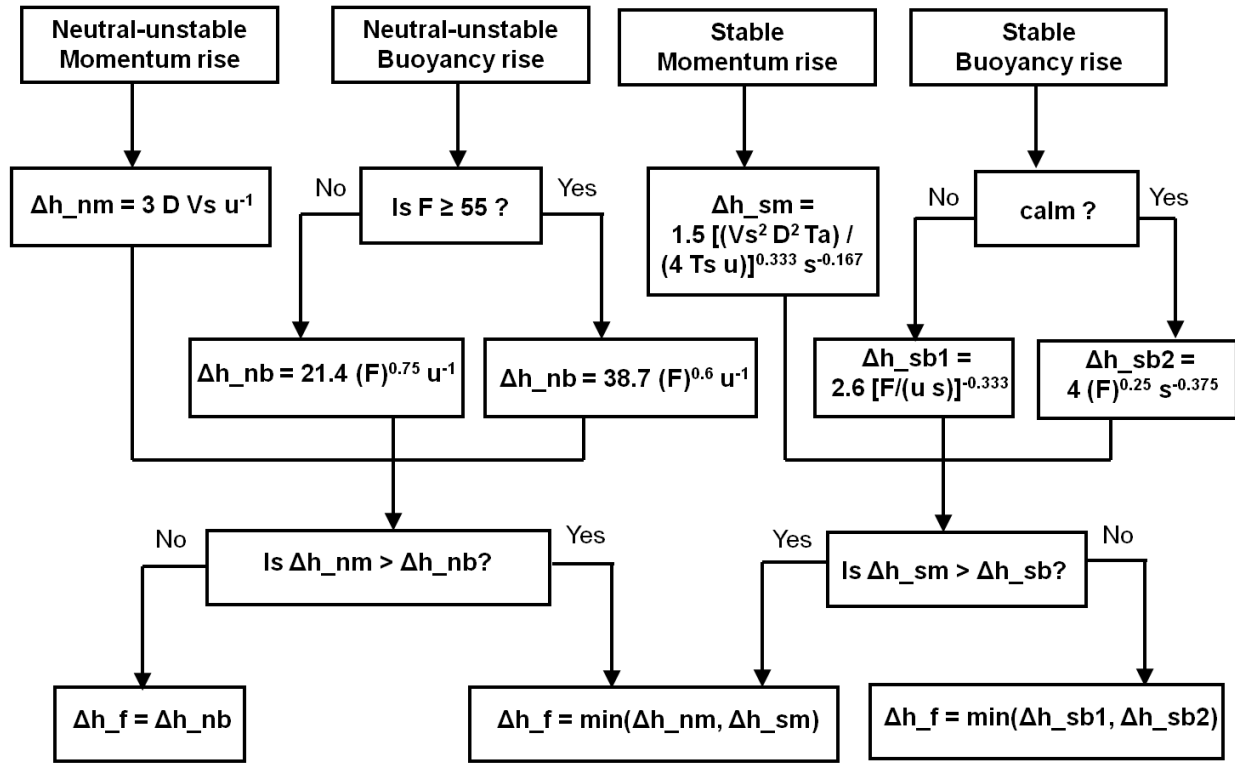


**Figure S1:** Logic diagram of the 'NILU Plume' algorithm to obtain final plume rise. In the diagram,  $F$  is the buoyancy factor (in  $\text{m}^4 \text{s}^{-3}$ ),  $V_s$  is stack exit velocity (in  $\text{m s}^{-1}$ ),  $D$  is stack diameter (in  $\text{m}$ ),  $T_a$  is ambient temperature (in  $\text{K}$ ),  $T_s$  is exhaust gas temperature (in  $\text{K}$ ),  $u$  is wind speed at actual stack height (in  $\text{m s}^{-1}$ ), and  $s$  is the stability parameter (in  $\text{s}^{-2}$ ).

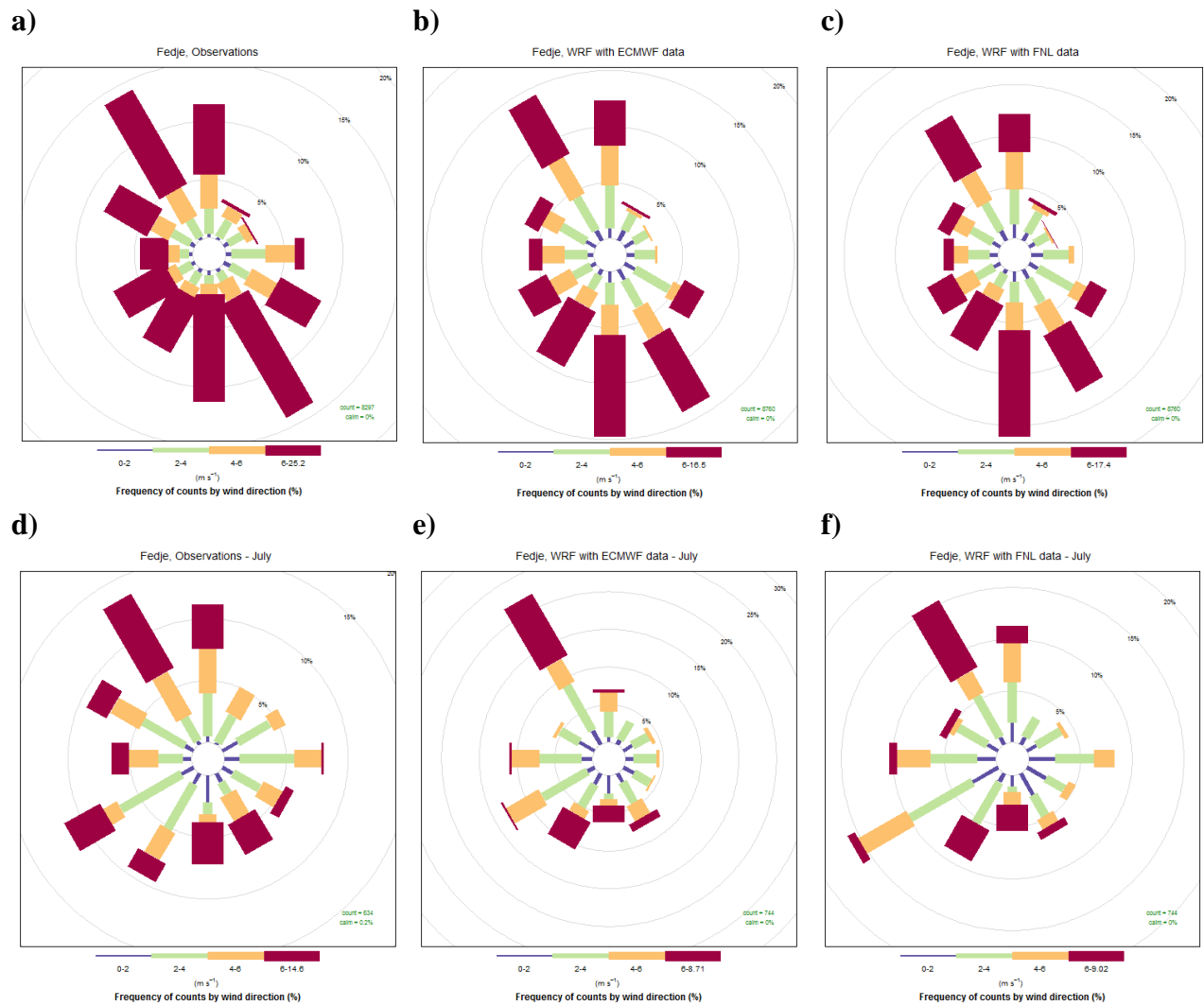


**Figure S2:** Comparison of wind roses for the year 2007 and for July 2007 at Fedje station [60.78°N; 4.72°E; 19 m a.s.l.]: a) annual wind rose based on observations, b) annual wind rose based on WRF model with ECMWF met data, c) annual wind rose based on WRF model with NCEP FNL data, d) July wind rose based on observation, e) July wind rose based on WRF model with ECMWF, and f) July wind rose based on WRF model with NCEP FNL data.

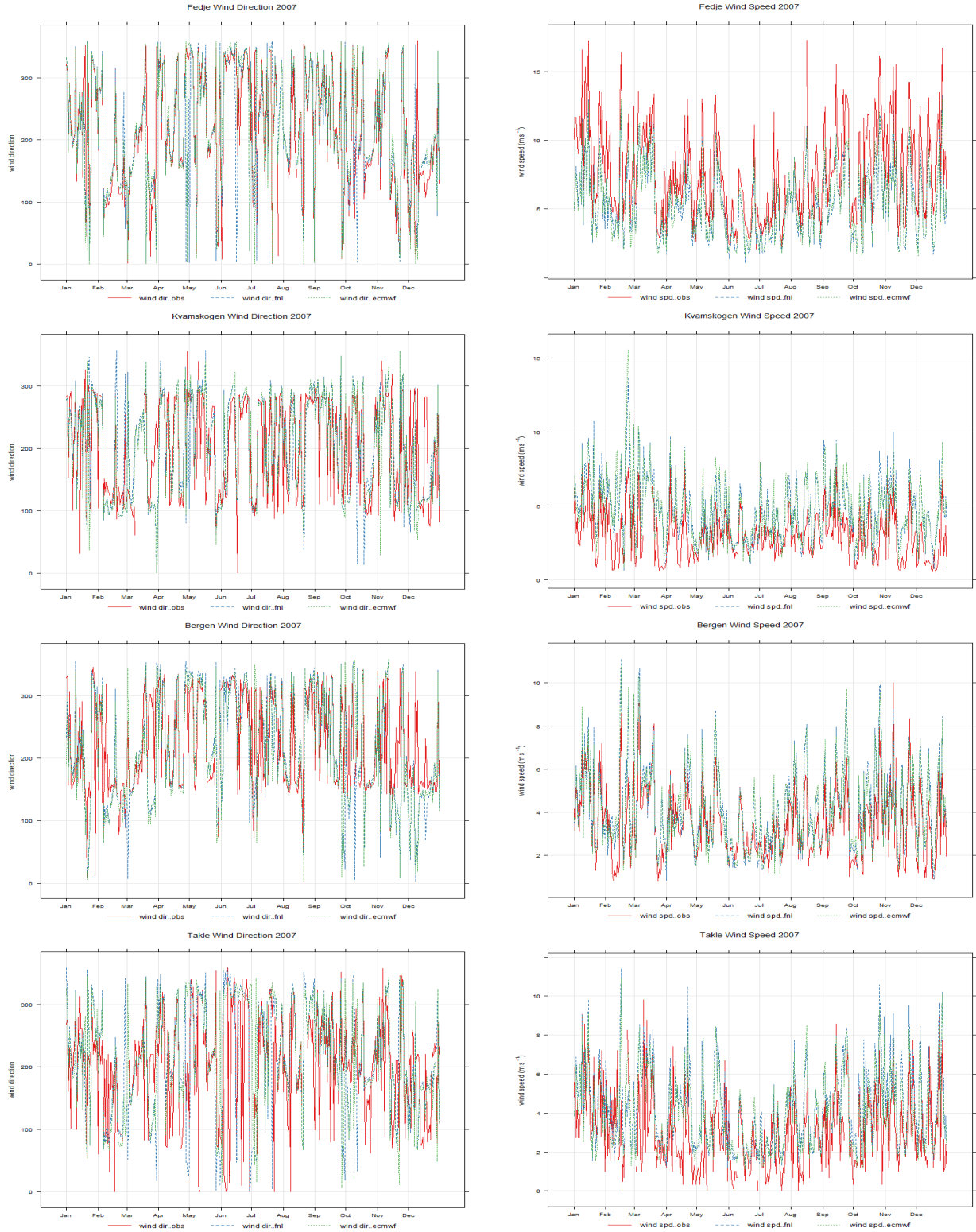


**Figure S3:** Comparison of wind direction (left column) and wind speed (right column) time series for 2007 at Fedje, Kvamskogen, Bergen and Takle based on daily average intervals from observation (red line) and WRF model with ECMWF data (green dashed line) and WRF model with NCEP FNL data (blue dashed line).

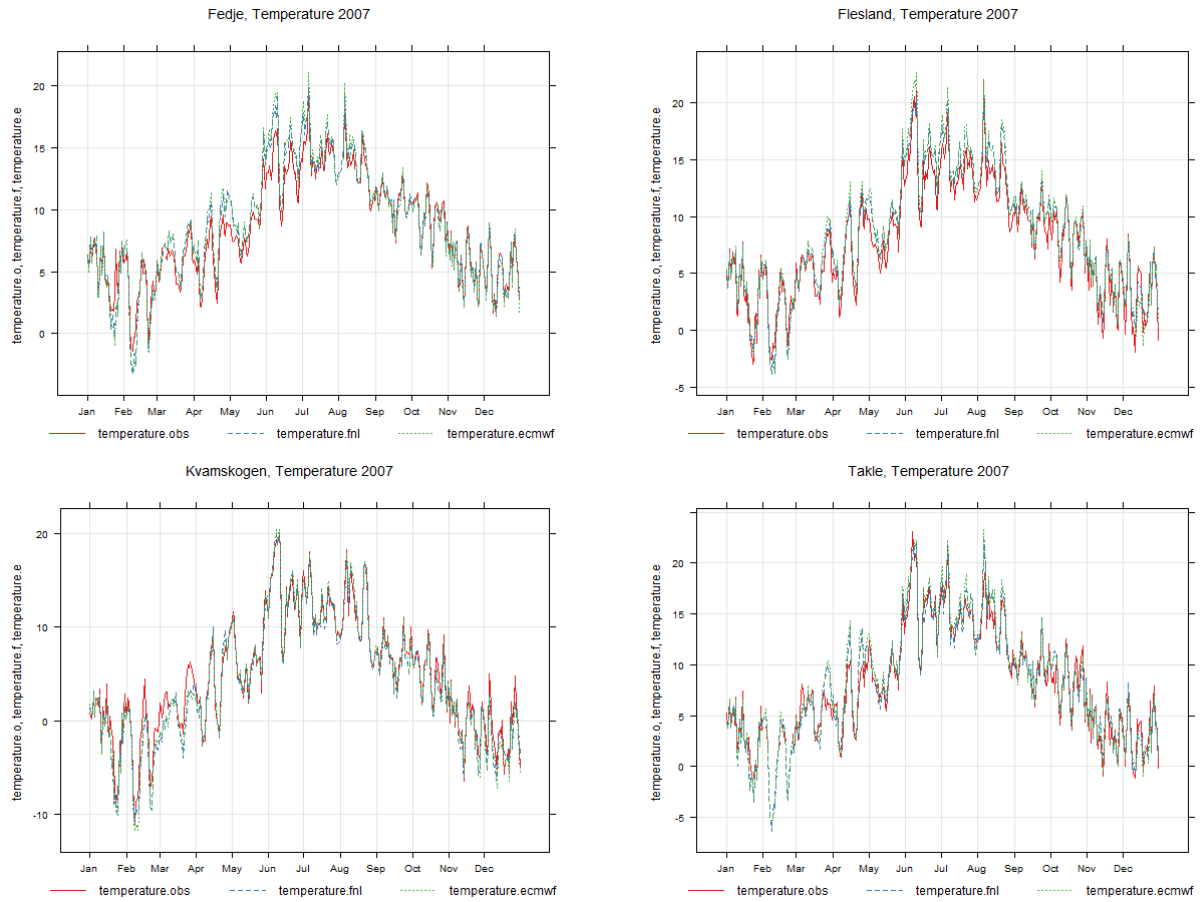
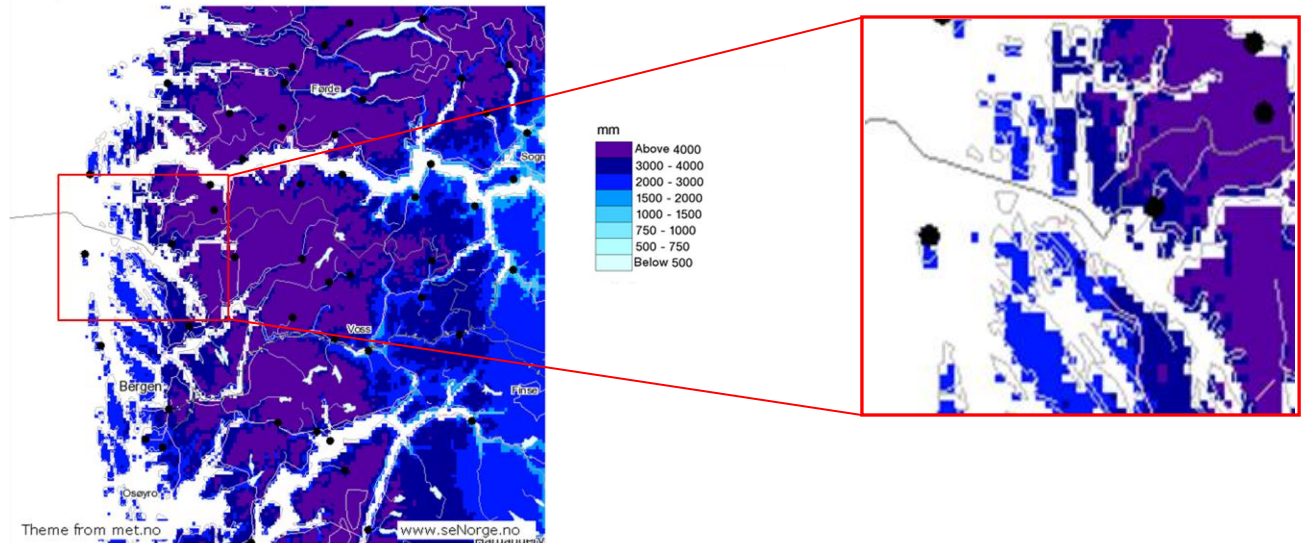


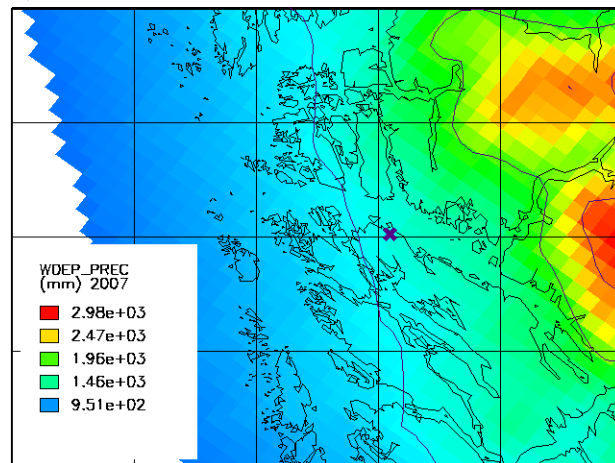
**Figure S4:** Comparison of temperature time series for 2007 at Fedje, Flesland, Kvamskogen, and Takle based on daily average intervals from observation (red line), WRF model with ECMWF data (green dashed line) and WRF model with NCEP FNL data (blue dashed line).

a)

Precipitation annual total (2007)



b)



c)

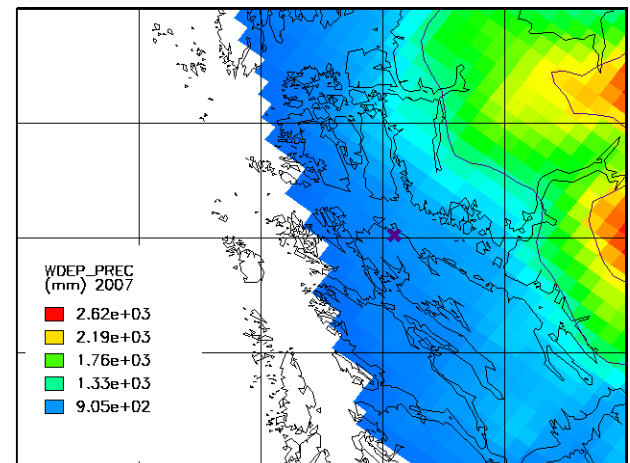
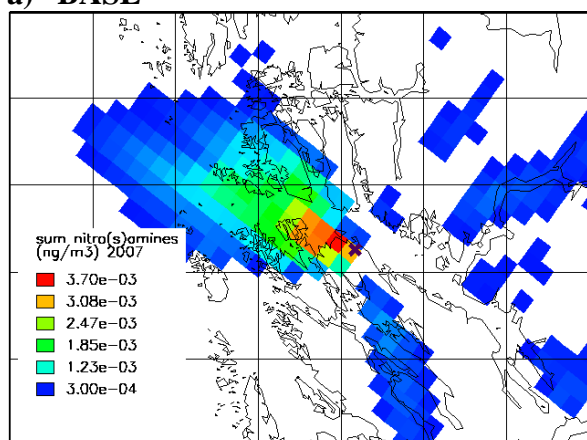
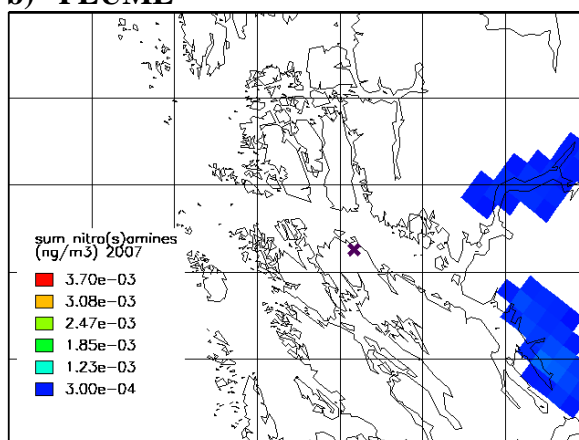


**Figure S5:** Total annual precipitation amount (as rain and snow) in 2007: a) map generated based on precipitation measurements from the Norwegian Meteorological Institute (available at <http://noserge.no>), red square showing approximate extend of the study area, a zoom into the area is shown to the right, b) precipitation map based on WRF model with ECMWF met data, and c) precipitation map based on WRF model with NCEP FNL data. The modelled total precipitation amount with NCEP FNL met data is uniformly 10-15% lower than with ECMWF met data.

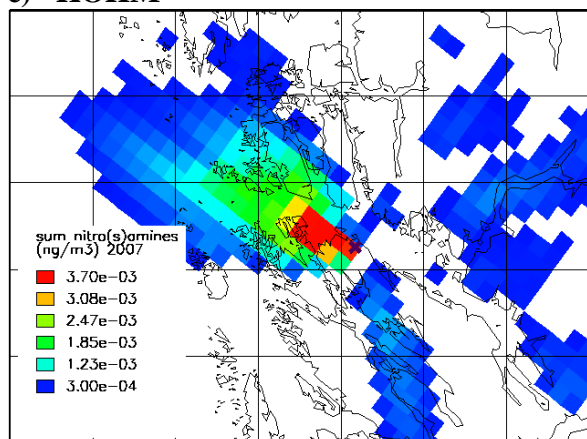
**a) BASE**



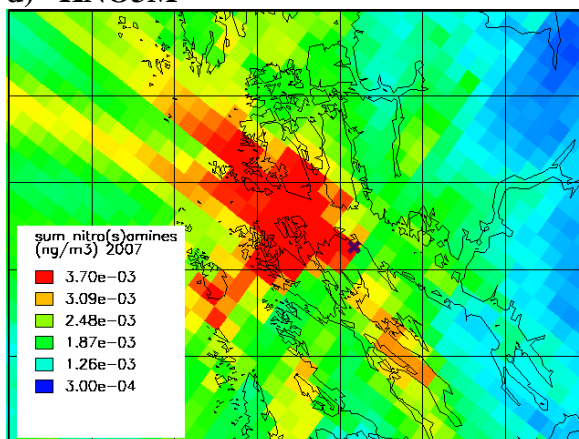
**b) PLUME**



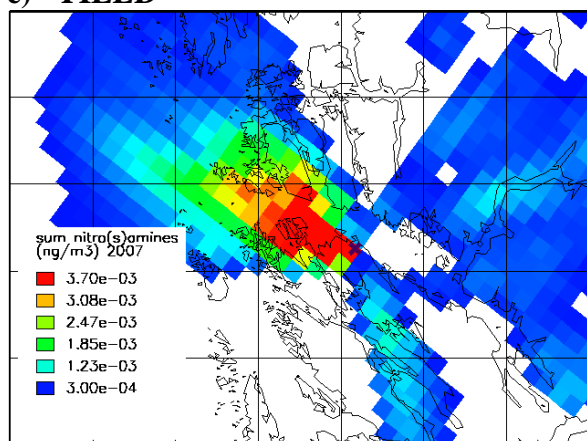
**c) KOHM**



**d) KNO3M**



**e) YIELD**



**f) KNIM**

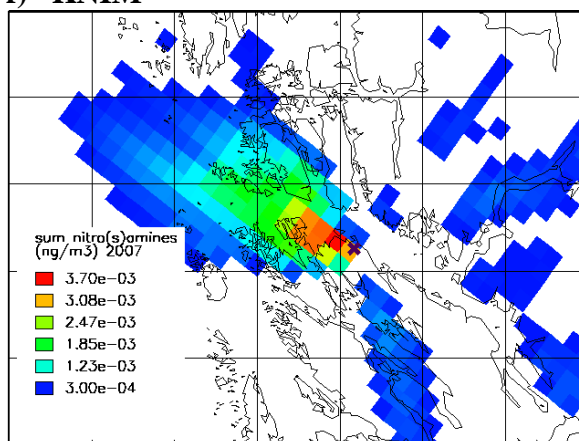
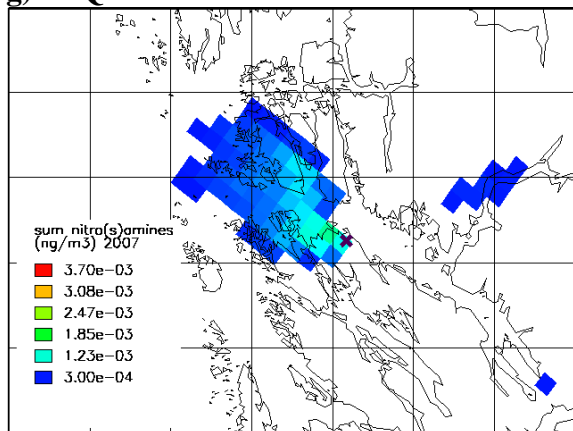


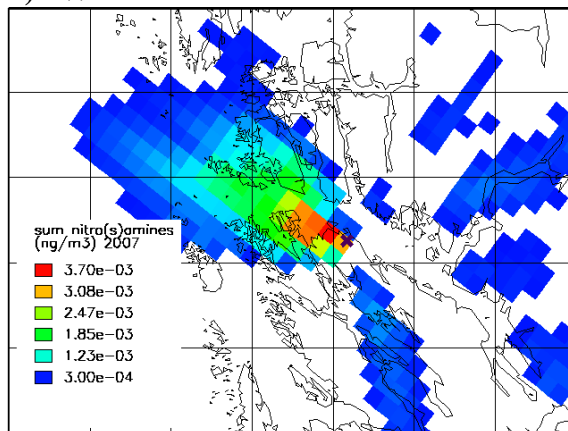
**Figure S6: Continued.**



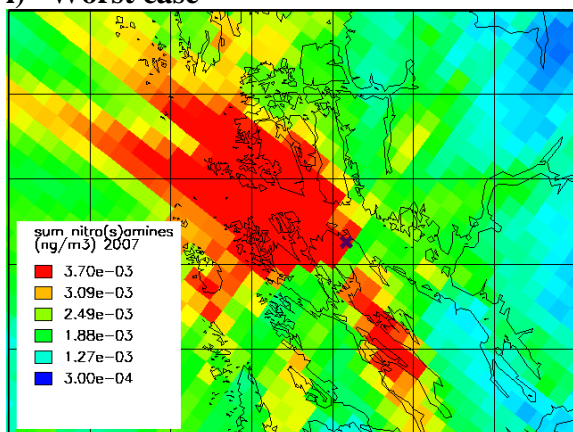
g) AQP



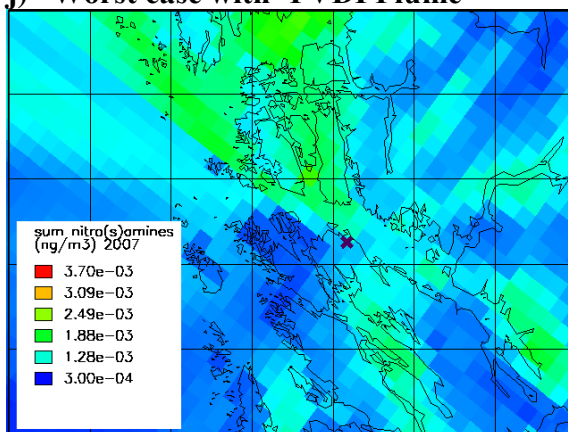
h) WDEP



i) Worst case



j) Worst case with 'PVDI Plume'



k) NCEP

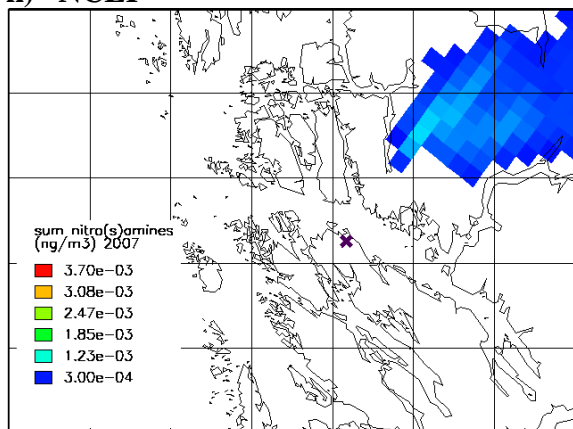
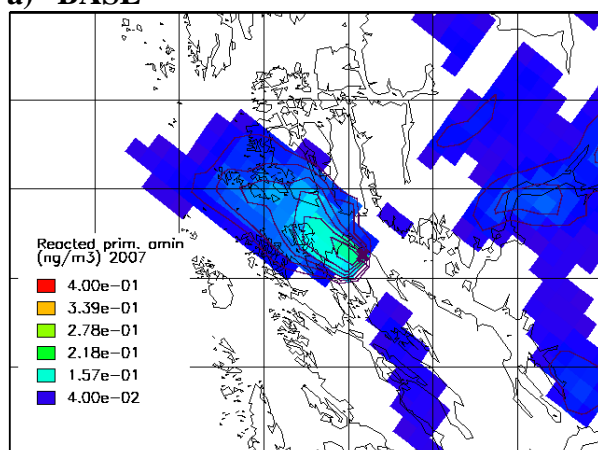


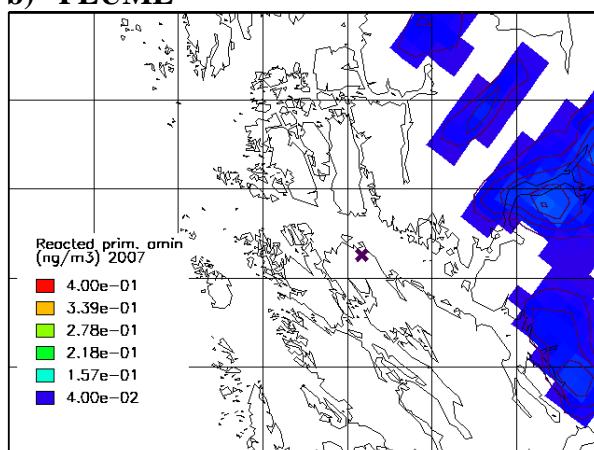
**Figure S6:** Air concentration of the sum of nitrosamines and nitramines (in  $\text{ng m}^{-3}$ ) at ground level. Spatial distribution of the annual average (year 2007) computed by WRF-EMEP in a) case BASE, b) case PLUME, c) case KOHM, d) case KNO3M, e) case YIELD, f) case KNIM, g) case AQP, h) case WDEP, i) Worst case, j) Worst case with 'PVDI Plume', and k) Baseline case using NCEP FNL met data. Values below the smallest legend entry are not shown. Plots have the same concentration scale with an upper cut-off at  $3.7 \times 10^{-3} \text{ ng m}^{-3}$  for better comparability. The location of CCP Mongstad is marked by a purple X. The grid cells divided by black lines illustrate an extent of  $10 \times 10 \text{ km}^2$ .



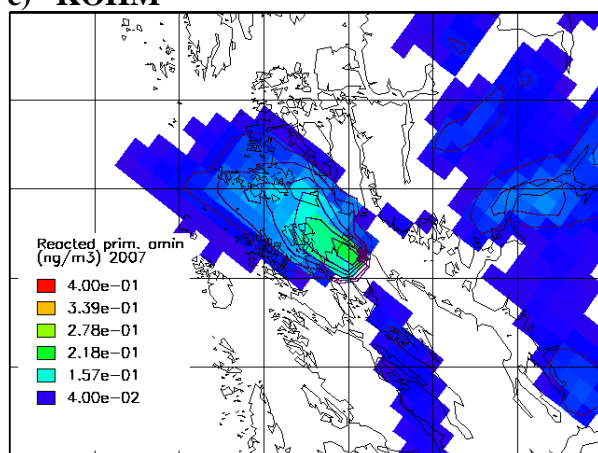
a) BASE



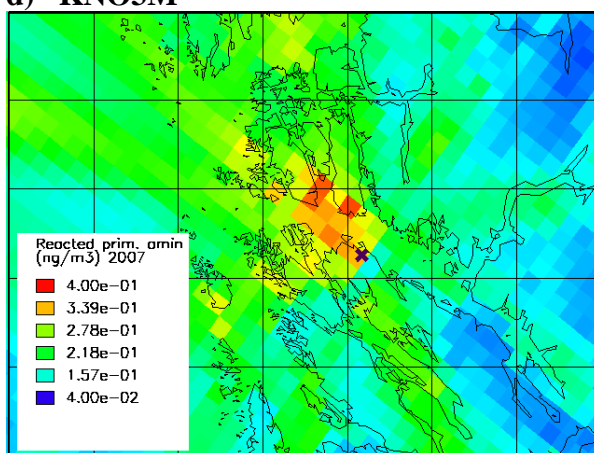
b) PLUME



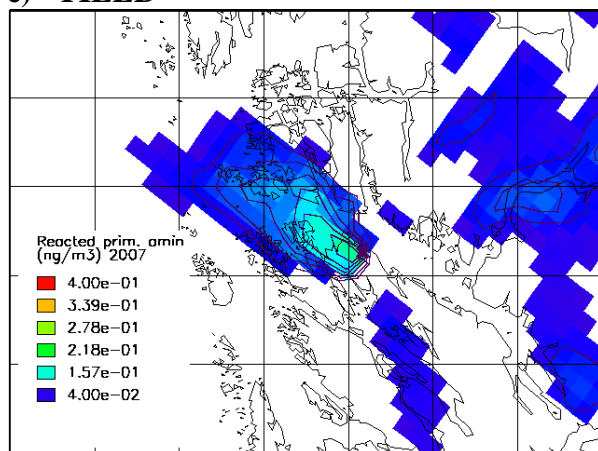
c) KOHM



d) KNO3M



e) YIELD



f) KNIM

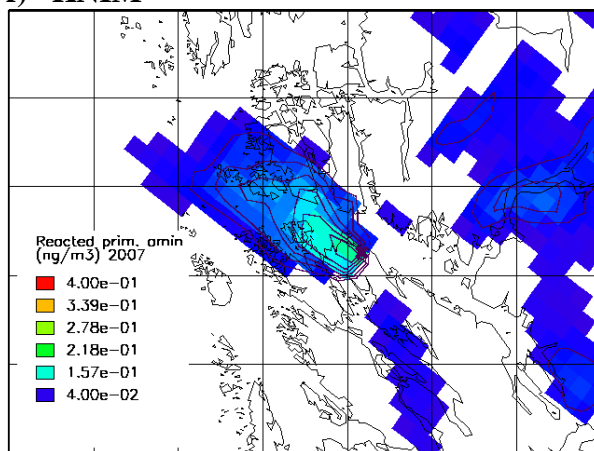
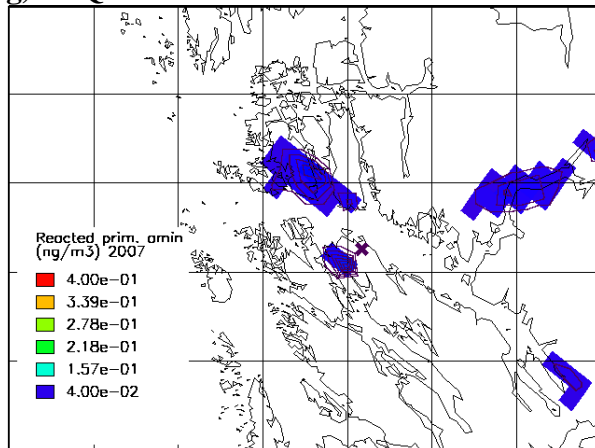
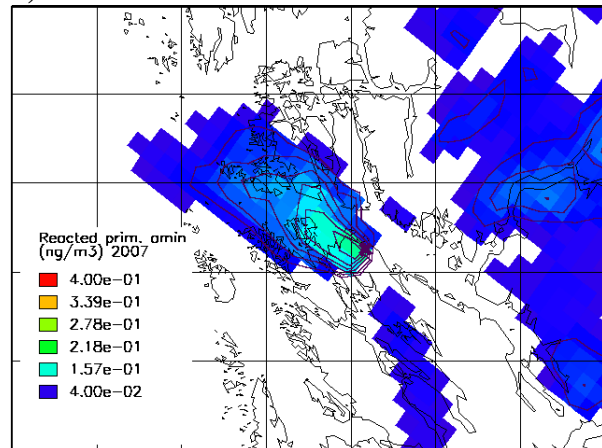


Figure S7: Continued.

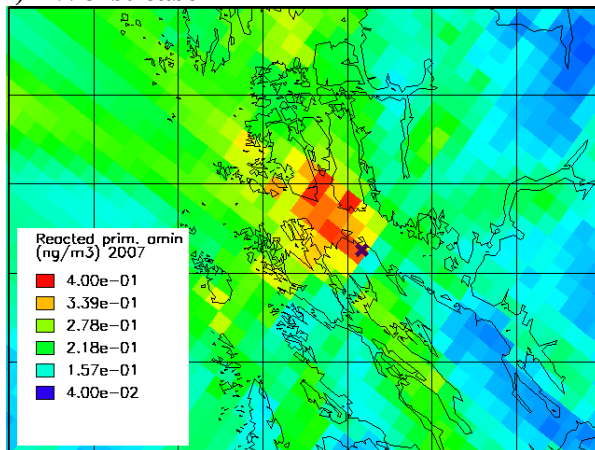
g) AQP



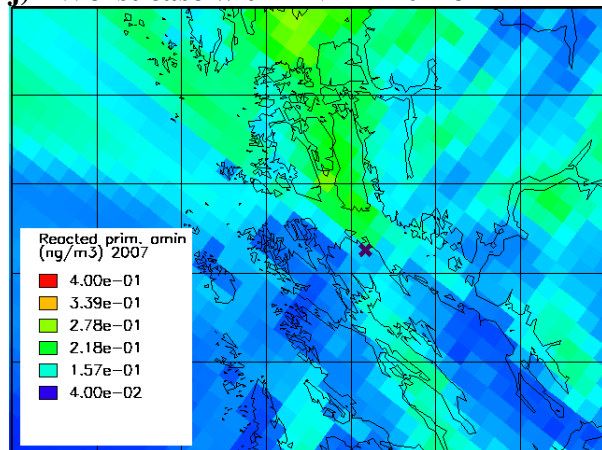
h) WDEP



i) Worst case



j) Worst case with 'PVDI Plume'



k) NCEP

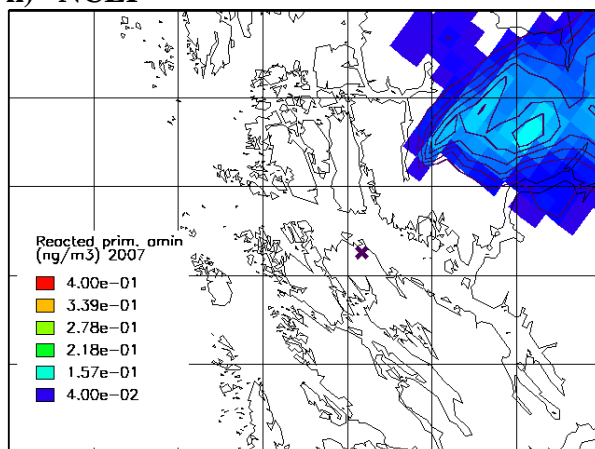


**Figure S7:** Reacted amount of MEA at ground-level on annual average (year 2007) expressed as concentration difference (in  $\text{ng m}^{-3}$ ) for: a) case BASE, b) case PLUME, c) case KOHM, d) case KNO3M, e) case YIELD, f) case KNIM, g) case AQP, h) case WDEP, i) Worst case, j) Worst case with 'PVDI Plume', and k) Baseline case using NCEP FNL met data. All plots have the same scale. Values below the smallest legend entry are not shown. The location of CCP Mongstad is marked by a purple X. The grid cells divided by black lines illustrate an extent of  $10 \times 10 \text{ km}^2$ .

WRF Mongstad July 2007 Wind rose layers 1-6

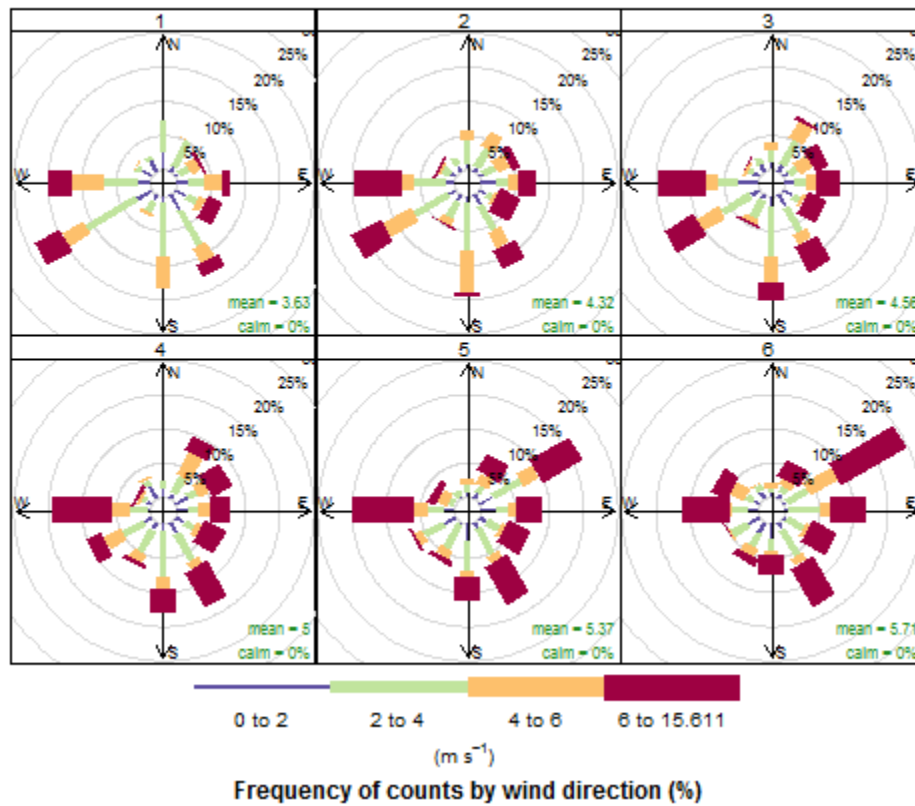
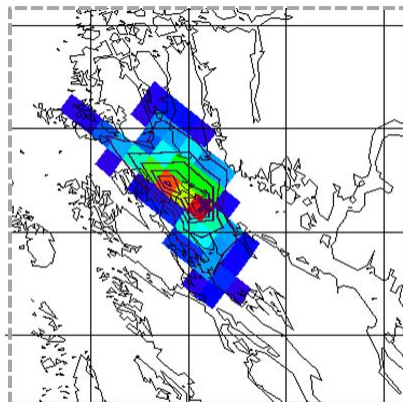
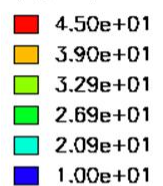


**Figure S8:** Wind roses for the six lowermost layers in the WRF model (up to ~1117 m) at location CCP Mongstad for July 2007, based on ECMWF met data. In layer 3 (184-324 m) highest wind speeds occur for wind directions 100°-150° and around 250°. On average, a certain shift in the wind speed and direction from the lowermost layer up to the top (sixth) layer is notable, with less wind coming from south-west - and more coming from north-east - in the upper layers.

a)

AMINE  
(ng/m<sup>3</sup>) 2007



b)

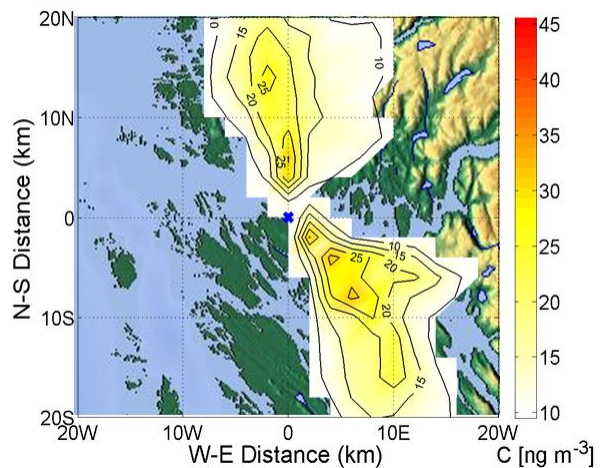


**Figure S9:** Comparison of the annual average (year 2007) ground-level air concentration of a chemically inert tracer (in ng m<sup>-3</sup>) emitted from the CCP with unity emission rate (1 g s<sup>-1</sup>) from a) the WRF-EMEP simulation (reference scenario) and b) the TAPM simulation of the worst case scenario study by Karl et al. (2011). The same concentration scale is used for both maps. Concentration values below 10 ng m<sup>-3</sup> are not shown. The location of CCP Mongstad is marked by a blue X. The grid cells divided by black lines illustrate an extent of 10x10 km<sup>2</sup>.

## References

ASME, American Society of Mechanical Engineers, Recommended Guide for the Prediction of the Dispersion of Airborne Effluents, 2nd ed., ASME, New York, U.S.A., 1973.

Briggs, G. A.: Some recent analyses of plume rise observation, In: Proceedings of the Second International Clean Air Congress, Ed. H. M. Englund and W. T. Berry, Academic Press, Washington, U.S.A., pp. 1029-1032, 1971.

Karl, M., Wright, R. F., Berglen, T. F., and Denby, B.: Worst case scenario study to assess the environmental impact of amine emissions from a CO<sub>2</sub> capture plant, *Int. J. Greenhouse Gas Control*, 5, 439-447, 2011.

Kuenen, J., Denier van der Gon, H., Visschedijk, A., and van der Brugh, H.: High resolution European emission inventory for the years 2003 - 2007, TNO report TNO-060-UT-2011-00588, Utrecht, Netherlands, 2011.

Pregger, T. and Friedrich, R., Effective pollutant emission heights for atmospheric transport modelling based on real-world information, *Environmental Pollution*, 157, 552-560, 2009.

Schaap, M., Hendriks, C., Kranenburg, R., Cuvelier, C., Thunis, P., Fagerli, H., Simpson, D., Schulz, M., Colette, A., Terrenoire, E., Bessagnet, B., Rouil, L., Stern, R., and Graff, A.: Performance of European chemistry transport models as function of horizontal resolution, [http://www.unece.org/fileadmin/DAM/env/documents/2012/air/EMEP\\_36th/N\\_10\\_Performance\\_of\\_European\\_chemistry\\_transport\\_models\\_as\\_function\\_of\\_horizontal\\_resolution\\_14\\_sep\\_2012.pdf](http://www.unece.org/fileadmin/DAM/env/documents/2012/air/EMEP_36th/N_10_Performance_of_European_chemistry_transport_models_as_function_of_horizontal_resolution_14_sep_2012.pdf), 2012 (accessed December 10, 2013)

Seinfeld, J. H. and Pandis, S. N., Ch. 18.5 Plume Rise, In: *Atmospheric Chemistry and Physics, From Air Pollution to Climate Change*, pp. 931-933, John Wiley & Sons Inc., New York, U.S.A., 1998.

Simpson, D., Benedictow, A., Berge, H., Bergström, R., Emberson, L. D., Fagerli, H., Flechard, C. R., Hayman, G. D., Gauss, M., Jonson, J. E., Jenkin, M. E., Nyíri, A., Richter, C., Semeena, V. S., Tsyro, S., Tuovinen, J.-P., Valdebenito, Á., and Wind, P.: The EMEP MSC-W chemical transport model – technical description, *Atmos. Chem. Phys.*, 12, 7825-7865, 2012.

VDI: Ausbreitung von Luftverunreinigungen in der Atmosphäre; Berechnung der Abgasfahnen-überhöhung. (Dispersion of air pollutants in the atmosphere; determination of plume rise) 1985-06 (German/English), Kommission Reinhaltung der Luft (KRdL) im VDI und DIN – Normenausschuss, 1985, Available from: <http://www.vdi.de>, (accessed December 10, 2013)

Yiannoukas, S., Morale, G., Williams, R., and Johnson, A.: Deposition and soil transport modelling of components from postcombustion amine-based CO<sub>2</sub> capture, Report for Gassnova SF. Det Norske Veritas Ltd, UK, Report No. PP011015, London, U.K., 2011. Available at: [http://www.gassnova.no/gassnova2/frontend/files/CONTENT/Rapporter/Depositionandsoiltransportmodelling\\_DNV.pdf](http://www.gassnova.no/gassnova2/frontend/files/CONTENT/Rapporter/Depositionandsoiltransportmodelling_DNV.pdf), (accessed December 10, 2013).